Geminate Processes in the Reaction of Nitric Oxide with 1-Methylimidazole–Iron(II) Porphyrin Complexes. Steric, Solvent Polarity, and Viscosity Effects

Teddy G. Traylor,* Douglas Magde, James Marsters, Karen Jongeward, Guo-Zhang Wu, and Kevin Walda

Contribution from the Department of Chemistry, 0506, University of California, San Diego, 9500 Gilman Drive, La Jolla, California 92093-0506

Received December 11, 1992

Abstract: The quantum yields for photolysis of imidazole–iron(II) porphyrin–NO complexes have been determined in the following solvents: toluene, aqueous 1-methylimidazole, Nujol, and glycerol. The corresponding yields are 0.2, 0.077 (30% 1-methylimidazole in water), 0.064, and 0.007. Steric effects on NO photolysis were also investigated. The increasingly hindered porphyrins (mesoheme, anthracene-7,7-cyclophane heme, adamantane-6,6-cyclophane heme, and pyridine-5,5-cyclophane heme) had, in toluene, quantum yields of 0.21, 0.23, 0.29, and 0.49, respectively. Several conclusions are drawn from these results. (1) Polar solvents decrease NO quantum yields. (2) Considering the enormous differences in ligand association rates, increased steric effects have relatively little influence. This is in accord with previous studies on isocyanides. (3) As is expected from a consideration of cage effects, increased viscosity reduces quantum yield. The relevance of these findings to heme protein reactions is discussed.

Introduction

Fast kinetic measurements of photolyses of heme proteins and their model compounds have revealed interesting geminate return processes which are important in understanding the mechanistic control of oxygen binding and delivery.[1-9]

Our recent studies of alkyl isocyanide recombinations following photolysis of heme or heme protein complexes[9a,10] indicated a three-state dissociation mechanism for hemes (eq 1) and corroborated the previously proposed[2a,c,e] four-state mechanism for myoglobin (eq 2).

$$\mathrm{BHm\,CNR} \underset{k_{-1}}{\overset{h\nu,\ k_1}{\rightleftharpoons}} \mathrm{[BHm\ CNR]} \underset{k_{-2}}{\overset{k_2}{\rightleftharpoons}} \mathrm{BHm + RNC} \qquad (1)$$

$$\mathrm{Mb\,CNR} \underset{k_{-1}}{\overset{h\nu,\ k_1}{\rightleftharpoons}} \mathrm{[Mb\ CNR]} \underset{k_{-2}}{\overset{k_2}{\rightleftharpoons}} \mathrm{[Mb\,\|\,CNR]} \underset{k_{-3}}{\overset{k_3}{\rightleftharpoons}} \mathrm{Mb + RNC} \qquad (2)$$

We have since demonstrated the effects of pressure,[11] solvent viscosity,[10a] the size of RNC,[10a] and steric hindrance[9c] on geminate reactions. These results are consistent with the three-state model for simple hemes and strongly support four-state protein models, at least for isocyanides as ligands. In particular, we observed that k_{-1} and k_2 were almost identical for *t*-BuNC return in myoglobin, horseradish peroxidase, and the model, chelated protoheme.[9b,d] This prompted the suggestion[9d] that the bond-making step ("innermost barrier")[2a] is devoid of steric hindrance in proteins.

There is some disagreement concerning mechanisms of ligation control in proteins because X-ray crystallography data[12] and several equilibrium and kinetic studies have been interpreted as evidence that the bound state and the transition state leading to the bound state suffer severe steric hindrance.[13-21] Two explanations are apparent: (1) the steric effects on CO rebinding to

(1) Duddell, D. A.; Morris, R. J.; Richards, J. T. *J. Chem. Soc., Chem. Commun.* **1979**, 75–76.

(2) (a) Alberding, N.; Austin, R. H.; Chan, S. S.; Eisenstein, L.; Frauenfelder, H.; Good, D.; Kaufmann, K.; Marden, M.; Nordlund, T. M.; Reinisch, L.; Reynolds, A. H.; Sorenson, L. B.; Wagner, G. C.; Yue, K. T. *Biophys. J.* **1978**, *24*, 319–334. (b) Marden, M. C. *Eur. J. Biochem.* **1982**, *128*, 399–404. (c) Ansari, A.; DiIorio, E. E.; Dlott, D. D.; Frauenfelder, H.; Iben, I. E. T.; Langer, P.; Roder, H.; Sauke, T. B.; Shyamsunder, E. *Biochemistry* **1986**, *25*, 3139–3146. (d) Frauenfelder, H.; Nienhaus, G. U.; Johnson, J. B. *Ber. Bunsen-Ges. Phys. Chem.* **1991**, *95*, 272–278. (e) Doster, W.; Bowne, S. F.; Frauenfelder, H.; Reinisch, L.; Shyamsunder, E. *J. Mol. Biol.* **1987**, *194*, 299–312. (f) Austin, R. H.; Beeson, K. W.; Eisenstein, L.; Frauenfelder, H.; Gunsalus, I. C. *Biochemistry* **1975**, *14*, 5355–5373.

(3) (a) Postlewaite, J. C.; Miers, J. B.; Dlott, D. D. *J. Am. Chem. Soc.* **1989**, *111*, 1248–1255. (b) Miers, J. B.; Postlewaite, J. C.; Cowen, B. R.; Roemig, G. R.; Lee, I.-Y. S.; Dlott, D. D. *J. Chem. Phys.* **1991**, *94*, 1825–1836. (c) Miers, J. B.; Postlewaite, J. C.; Zyung, T.; Chen, S.; Roemig, G. R.; Wen, X.; Dlott, D. D.; Szabo, A. *J. Chem. Phys.* **1990**, *93*, 8771–8776.

(4) (a) Greene, B. I.; Hochstrasser, R. M.; Weisman, R. B.; Eaton, W. A. *Proc. Natl. Acad. Sci. U.S.A.* **1978**, *75*, 5255–5259. (b) Henry, E. R.; Eaton, W. A.; Hochstrasser, R. M. *Proc. Natl. Acad. Sci. U.S.A.* **1986**, *83*, 8982–8986. (c) Henry, E. R.; Sommer, J. H.; Hofrichter, J.; Eaton, W. A. *J. Mol. Biol.* **1983**, *166*, 443–451. (d) Moore, J. N.; Hansen, P. A.; Hochstrasser, R. M. *Chem. Phys. Lett.* **1987**, *138*, 110–114. (e) Anfinrud, P. A.; Han, C.; Hochstrasser, R. M. *Proc. Natl. Acad. Sci. U.S.A.* **1989**, *86*, 8387–8391.

(5) (a) Marden, M. C.; Hazard, E. S., III; Gibson, Q. H. *Biochemistry* **1986**, *25*, 2786–2792. (b) Rohlfs, R. J.; Olson, J. S.; Gibson, Q. H. *J. Biol. Chem.* **1988**, *263*, 1803–1813.

(6) (a) Petrich, J. W.; Poyart, C.; Martin, J.-L. *Biochemistry* **1988**, *27*, 4049–4060. (b) Martin, J.-L.; Migus, A.; Poyart, C.; Lecarpentier, Y.; Astier, R.; Antonetti, A. *Proc. Natl. Acad. Sci., U.S.A.* **1983**, *80*, 173–177.

(7) Momenteau, M.; Loock, B.; Tetreau, C.; Lavallette, D.; Croisy, A.; Shaeffer, C.; Huel, C.; Lhoste, J.-M. *J. Chem. Soc., Perkin Trans. 2* **1987**, 249–257.

(8) Chance, M. R.; Courtney, S. H.; Chavez, M. D.; Ondrias, M. R.; Friedman, J. M. *Biochemistry* **1990**, *29*, 5537–5545.

(9) (a) Traylor, T. G.; Magde, D.; Taube, D. J.; Jongeward, K. A. *J. Am. Chem. Soc.* **1987**, *109*, 5864–5865. (b) Jongeward, K. A.; Magde, D.; Taube, D. J.; Marsters, J. C.; Traylor, T. G.; Sharma, V. S. *J. Am. Chem. Soc.* **1988**, *110*, 380–387. (c) Traylor, T. G.; Taube, D. J.; Jongeward, K. A.; Magde, D. *J. Am. Chem. Soc.* **1990**, *112*, 6875–6880. (d) Traylor, T. G.; Magde, D.; Taube, D. J.; Jongeward, K. A.; Bandyopadhyay, D.; Luo, J.; Walda, K. N. *J. Am. Chem. Soc.* **1992**, *114*, 417–429. (e) Taube, D. J.; Traylor, T. G.; Magde, D.; Walda, K. N.; Luo, J. *J. Am. Chem. Soc.* **1992**, *114*, 9182–9188. (f) Bandyopadhyay, D.; Magde, D.; Traylor, T. G.; Sharma, V. S. *Biophys. J.* **1992**, *63*, 673–681.

(10) (a) Traylor, T. G.; Magde, D.; Luo, J., manuscript in preparation. (b) Traylor, T. G.; Magde, D.; Sharma, V. S.; Bandyopadhyay, D.; Walda, K. N., manuscript in preparation.

(11) Traylor, T. G.; Luo, J.; Simon, J. A.; Ford, P.C. *J. Am. Chem. Soc.* **1992**, *114*, 4340–4345.

(12) (a) Baldwin, J. *J. Mol. Biol.* **1980**, *136*, 103–128. (b) Jameson, G. B.; Molinaro, F. S.; Ibers, J. A.; Collman, J. P.; Brauman, J. I.; Rose, E.; Suslick, K. S. *J. Am. Chem. Soc.* **1980**, *102*, 3224–3237. (c) Deatherage, J. F.; Loe, R. S.; Anderson, C. M.; Moffat, K. *J. Mol. Biol.* **1976**, *104*, 687–706. (d) Deatherage, J. F.; Loe, R. S.; Moffat, K. *J. Mol. Biol.* **1976**, *104*, 723–728.

(13) Makinen, M. W.; Houtchens, R. A.; Caughey, W. S. *Proc. Natl. Acad. Sci. U.S.A.* **1979**, *76*, 6042–6046.

(14) (a) Collman, J. P.; Brauman, J. I.; Doxsee, K. M.; Halbert, T. R.; Suslick, K. S. *Proc. Natl. Acad. Sci. U.S.A.* **1978**, *75*, 564–568. (b) Collman, J. P.; Brauman, J. I.; Doxsee, K. M. *Proc. Natl. Acad. Sci. U.S.A.* **1979**, *76*, 6035–6039. (c) Collman, J. P. *Acc. Chem. Res.* **1977**, *10*, 265–272.

0002-7863/93/1515-4808$04.00/0

hemes occur before the bond-making step or (2) isocyanides are special molecules which do not behave as do small molecules such as CO or O_2.

The geminate rebinding of nitric oxide after picosecond photolyses of heme protein–NO complexes is now well established.[22-24] Geminate rate constants do not differ much from those of isocyanides. In addition, the bimolecular rate constant for model compounds (BHm) reacting with NO is 2×10^8 M^{-1} s^{-1},[21,25] very close to the rate constants for isocyanides,[26] imidazoles,[9c] pyridines,[27] and ethers,[28] and is indicative of a diffusion-controlled reaction. Since both NO and O_2 have very nearly diffusion-controlled reactions with models and both display observable picosecond recombination in myoglobin[9b,29] (whereas CO does not[4,9d]), it seemed to us that NO is a better small-molecule model for O_2 than is carbon monoxide. The quantum yield for photolysis of BHm–NO is around 0.07,[25] while that for hemoglobin–NO is less than 10^{-3}.[30] These findings are interpreted as strong indications of substantial geminate return.

In order to further document this conclusion and to probe the effects of viscosity, steric hindrance, and other structural and medium effects on the geminate behavior of diatomic molecules, we have studied the quantum yield for photolysis of BHm–NO as a function of structural and environmental changes. The results are strikingly similar to those previously obtained with isocyanides. We also report picosecond kinetic behavior after photolysis of a base–heme–NO complex.

Experimental Section

Materials. Rhodamine 590 and Rhodamine 575 laser dyes were purchased from Exiton and dissolved in absolute ethanol. The dye solution was cooled to 18 ± 2 °C using a Brinkman IC-2 recirculating bath containing a myristyltrimethylammonium bromide (5%) solution. Sample temperature was maintained at 20.0 ± 0.2 °C with a water-jacket cell-holder attached to a recirculating bath filled with 50% ethylene glycol/water. Silica gel (60–200 mesh, grade H) was obtained from Davison Chemical. Alumina (80–325 mesh) was purchased from MCB. Degassed solutions were prepared by bubbling argon (with a syringe needle) through a sealed vial of the liquid for at least 1 h.

Reagents. 1-Methylimidazole (Aldrich) was distilled from sodium metal and stored over activated molecular sieves (4 Å, MCB). Toluene (Mallinckrodt AR) was purified according to literature methods,[31] except that it was distilled from calcium hydride (Aldrich) and stored over activated 4-Å molecular sieves. Tetrahydrofuran (Aldrich) was distilled under argon from potassium/benzophenone. Pyridine (Aldrich) was distilled from calcium hydride under an argon atmosphere. The buffer solutions were prepared with [bis(2-hydroxyethyl)amino]tris(hydroxymethyl)methane (Eastman), sodium phosphate (Mallinckrodt), or tris(hydroxymethyl)amino methane (Eastman). Myristyltrimethylammonium bromide (MTAB, Alfa) was recrystallized twice from acetone. The following were used as received: Nujol (Plough); mesitaldehyde (Aldrich); zinc (20 mesh, Mallinckrodt); ferrous bromide (Alfa); glycerol (Aldrich); mercuric chloride (Mallinckrodt); imidazole (Aldrich); triethylamine (Aldrich); *tert*-butylisonitrile (Fluka); octadecyl bromide (Aldrich); 1,4,7,10,13,16-hexaoxacyclooctadecane (18-crown-6, Fluka); and 4,7,13,16,21,24-hexaoxa-1,10-diazabicyclo[8.8.8]hexacosane (Kryptofix-222, Fluka). Sodium hydrosulfite (sodium dithionite) was generously provided by Virginia Chemical Co.[32] and stored in small Teflon-capped vials at 4 °C until used.[33]

Compressed Gases. Argon gas (commercial grade, Linde Products) was passed through an oxygen scrubber (American Science Products) before use. Carbon monoxide gas (99.99%, Matheson) was used as received. Nitric oxide (98.19%, Matheson), which required the use of a stainless steel regulator (14M-660, Matheson), was first passed through an Ascarite-filled (Aldrich) glass column (10×600 mm^2) and then through a dry ice trap. Polyethylene tubing and stainless steel fittings were used for the nitric oxide purification apparatus where possible.

***N*-Octadecylimidazole.** Ten grams (0.15 mol) of imidazole and 49 g (0.15 mol) of octadecyl bromide were dissolved in freshly-distilled THF (50 mL) and refluxed (40 h) over anhydrous potassium carbonate (20 g) under an argon atmosphere. Chloroform (200 mL) was added, and the solution was filtered to remove excess salts. After removal of the solvent under vacuum, the product was dissolved in chloroform and purified on a column of silica gel with a 50:50 mixture of chloroform/hexanes (containing 1% triethylamine). The solvent was removed under vacuum, and the resulting solid was recrystallized from boiling hexanes, yielding 19 g (40%) of the product as soft white crystals. ^{1}H NMR ($CDCl_3$): 7.5 (s, 1 H), 7.0 (s, 1 H), 6.9 (s, 1 H), 4.0 (t, 2 H), 1.1-1.5 (m, 37 H).

Reducing Agents. Several methods were used to reduce the hemin samples prior to addition of the appropriate ligands. For aqueous samples, a saturated solution of sodium dithionite was prepared by adding a degassed sodium borate solution (200 μL, 0.05 M) to a sealed vial which had been thoroughly flushed with argon and which contained sodium dithionite (50 mg).

For nonaqueous solvents, the reducing agent was prepared as an 18-crown-6 complex in methanol. Sodium dithionite (10 mg), dry 18-crown-6 (50 mg), and a small stir bar were sealed in a vial and flushed with argon for a few minutes. Degassed methanol (500 μL) was added via syringe, and the solution was stirred vigorously (30 min) under positive argon pressure. The solution was used immediately. 2,2,2-Kryptofix was used in place of the 18-crown-6 with equally good results.

Zinc amalgam was also used for reduction in apolar solvents. The amalgam was thoroughly washed with degassed water (4×3 mL) to remove any remaining acidic and ionic impurities. Next, the amalgam was washed with degassed methanol (2×2 mL) and stored under oxygen-free toluene. The reductant was placed directly into the sample cell as described below. While reduction with sodium dithionite solution was nearly instantaneous, hemin solutions required stirring (3–4 h) with the amalgam before reduction was complete. Ferrous complexes prepared in this manner were exceptionally stable.

Heme Compounds. Mesoporphyrin dimethyl ester was prepared from mesoporphyrin (Porphyrin Products) according to literature methods.[34] Protohemin chloride (bovine, Sigma) and sperm whale metmyoglobin (Sigma) were used as received. *meso*-Tetraphenylporphyrin was purchased from Sigma. Tetramesitylporphyrin was prepared according to literature methods.[35] Iron was inserted into the porphyrins according to standard procedures.[36] The cyclophane hemes from previous studies were used.[37]

Sample Preparation. For quantum yield determinations, heme samples were prepared in specially-designed tonometers as previously described.[37c]

Carbon Monoxide Complexes. Carboxymyoglobin was prepared by dissolving metmyoglobin (2 mg) in a sufficient amount of thoroughly degassed bis-tris buffer (pH 7, 0.05 M) containing NaCl (0.1 M) to give

(15) Moffatt, K. M.; Deatherage, J. F.; Seybert, D. W. *Science (Washington, DC)* **1979**, *206*, 1035–1042.
(16) Tucker, P. W.; Phillips, S. E. V.; Perutz, M. F.; Houtchens, R.; Caughey, W. S. *Proc. Natl. Acad. Sci. U.S.A.* **1978**, *75*, 1076–1080.
(17) (a) Reisberg, P. I.; Olson, J. S. *J. Biol. Chem.* **1980**, *255*, 4159–4169. (b) Olson, J. S.; McKinnie, R. E.; Mims, M. P.; White, D. K. *J. Am. Chem. Soc.* **1983**, *105*, 1522–1527. (c) Mims, M. P.; Porras, A. G.; Olson, J. S.; Noble, R. W.; Peterson, J. A. *J. Biol. Chem.* **1983**, *258*, 14219–14232.
(18) Jameson, G. B.; Ibers, J. A. *Comments Inorg. Chem.* **1983**, *2*, 97–126.
(19) Collman, J. P.; Brauman, J. I.; Iverson, B. L.; Sessler, J. L.; Morris, R. M.; Gibson, Q. H. *J. Am. Chem. Soc.* **1983**, *105*, 3052–3064.
(20) Mispelter, J.; Momenteau, M.; Lavalette, D.; Lhoste, J.-M. *J. Am. Chem. Soc.* **1983**, *105*, 5165–5166.
(21) Sharma, V. S.; Geibel, J. F.; Ranney, H. M. *Proc. Natl. Acad. Sci. U.S.A.* **1978**, *75*, 3747–3750.
(22) Cornelius, P. A.; Hochstrasser, R. M.; Steele, A. W. *J. Mol. Biol.* **1983**, *163*, 119–128.
(23) Petrich, J. W.; Lambry, J.-C.; Kuczera, K.; Karplus, M.; Poyart, C.; Martin, J.-L. *Biochemistry* **1991**, *30*, 3975–3987.
(24) Jongeward, K. A.; Marsters, J. C.; Magde, D. *Ultrafast Phenom. V* **1986**, *46*, 427–429.
(25) Rose, E. J.; Hoffman, B. M. *J. Am. Chem. Soc.* **1983**, *105*, 2866–2873.
(26) Taube, D. J.; Projahn, H. D.; van Eldik, R.; Magde, D.; Traylor, T. G. *J. Am. Chem. Soc.* **1990**, *112*, 6880–6886.
(27) Momenteau, M.; Lavalette, D. *J. Am. Chem. Soc.* **1978**, *100*, 4322–4324.
(28) Luo, J. Doctoral Dissertation, University of California, San Diego, CA 92109.
(29) Jongeward, K. A.; Marsters, J. C.; Mitchell, M. J.; Magde, D.; Sharma, V. S. *Biochem. Biophys. Res. Commun.* **1986**, *140*, 962–966.
(30) Antonini, E.; Brunori, M. *Hemoglobin and Myoglobin in Their Reactions with Ligands*; North-Holland Publishing Co.: Amsterdam, 1971; Vol. 21.
(31) (a) Riddick, J. A.; Bunger, W. B. *Organic Solvents. Physical Properties and Methods of Purification*, 3rd ed.; Wiley: New York, 1970; p 611. (b) Perrin, D. D.; Armaarego, W. L. F.; Perrin, D. R. *Purification of Laboratory Chemicals*; Pergamon Press: New York, 1966; p 143.
(32) Virginia Chemical Company, 3340 W. Norfolk Rd., Portsmouth, VA 23703.
(33) The use of very pure sodium dithionite is crucial for the preparation of this complex. Commonly available samples of this reagent from a number of suppliers were tested and found to be of insufficient purity.
(34) Falk, J. E. *The Porphyrins and Metalloporphyrins*; Elsevier Publishing Co.: New York, 1964; p 52.

a final protein concentration of 5×10^{-6} M. The sample was sealed in a tonometer, and the entire cell was flushed with carbon monoxide. Next, the hemin was reduced with saturated sodium dithionite (2 μL) in sodium borate (0.05 M) and stirred to form the carboxy complex.

The carbon monoxide complex of monochelated protoheme was prepared in a similar manner. The sample was prepared in bis-tris buffer (pH 7, 0.1 M) containing MTAB (2%) and degassed with three freeze–pump–thaw cycles prior to the addition of carbon monoxide and aqueous sodium dithionite.

Nitric Oxide Complexes. In a typical preparation, nitrosylmesoheme-1-methylimidazole was prepared in toluene in the following manner. A concentrated solution of mesohemin chloride dimethyl ester in chloroform was added via syringe to a solution of 1-methylimidazole (20%) in toluene to yield a hemin concentration of 3×10^{-5} M. A high concentration of 1-methylimidazole was necessary to ensure complete formation of the six-coordinate nitrosyl complex.[25,38] With the tonometer held horizontally, zinc amalgam (200 mg) was placed in the end of the cuvette section, and the hemin solution was transferred to the bulb section, which contained a small stir bar. The tonometer was sealed, the hemin solution was degassed with three freeze–pump–thaw cycles, and the sample was stored under an argon atmosphere. The amalgam was tipped into the hemin solution, and the sample was stirred until the absorbance spectrum showed that formation of the bis(1-methylimidazole)mesoheme complex was complete. Nitric oxide gas (10 mL, 1 atm) was introduced into the tonometer with a gas-tight syringe, and the sample was stirred (2 h) to yield a toluene solution of nitrosylmesoheme-1-methylimidazole.

Samples were prepared in other solvents in a similar manner. Hemin samples were dissolved in chloroform, methanol, or a methanol/50% sodium borate (0.05 M) buffer before being diluted with the desired solvent. Aqueous samples were reduced with saturated sodium dithionite solution (5 μL) in borate (0.05 M) and diluted into a sodium phosphate buffer (pH 9, 0.1 M) containing 1-methylimidazole (30%). High-viscosity experiments were performed in glycerol/buffer mixtures containing 1-methylimidazole (30% v/v) or in *N*-octadecylimidazole (0.3 M) in Nujol containing chloroform (10% v/v).

General Instrumentation. ^{1}H NMR spectra were recorded on a 90-MHz Varian EM-390 instrument. UV–visible spectra were recorded on a Kontron Uvicon 810 spectrophotometer which allowed digitization and storage of spectra on a VAX 11/750 computer via an RS-232 interface. pH measurements were made with a Corning Model 12 pH meter.

Photolysis Apparatus. Flash photolyses were performed with a Sunpak 611 photographic flash unit (pulse width ~0.5 ms) or a Phase-R Model DL 2100 AXH pulsed-dye laser (pulse width ~350 ns at 1.0 J). The photolytic pulse was directed onto the sample perpendicular to the analysis beam. The output of the flash unit was screened using a yellow glass filter (444-nm cutoff, Corning) to exclude UV light. The laser produced a pulse centered at 584 (Rhodamine 590) or 570 nm (Rhodamine 575). Intensity of the photolysis pulse was attentuated with suitable neutral-density filters.

Measurement of Flash Intensity. The intensity of the photographic flash was not determined directly. Instead, the relative flash intensity was computed from the transmittance of a neutral-density filter placed between the sample and the flash unit. Changing the filter allowed variation of the flash intensity over a factor of 10.

The output intensity of the laser was not sufficiently consistent for reliable determinations of the relative flash intensity in the same way. Instead, it was necessary to directly measure the intensity of each photolysis pulse using the apparatus described below. Ten percent of the laser output was diverted with a quartz flat (Melles-Griot) placed between the laser and the sample holder, with the flash directed onto the entrance slit of an EG&G 1229 monochromator attached to a Reticon photodiode array. The profile of the flash was recorded and its intensity measured by integration of the output from the diode array using an EG&G PAR Model 1215 system processor (Figure 1). The flash intensity, corrected for background noise, was determined for each photolytic event (Figure 2).

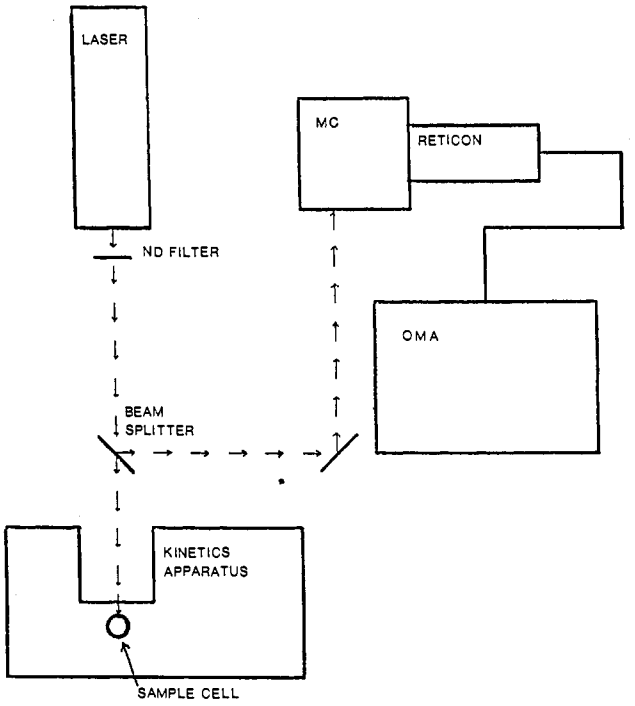

Figure 1. Schematic diagram of the apparatus used to measure photolysis quantum yields, including provision for monitoring the flash intensity of the laser pulse.

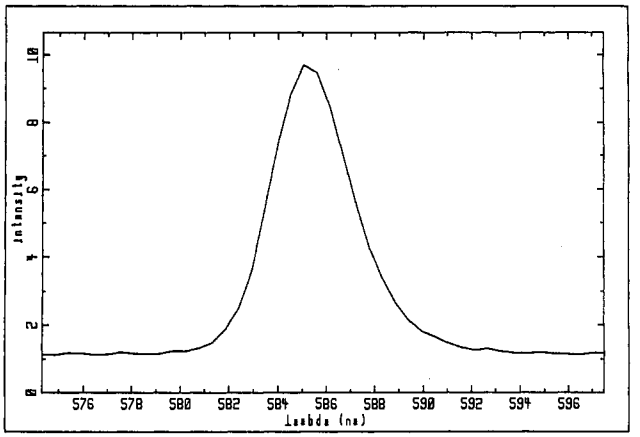

Figure 2. Intensity profile of the output from the pulsed-dye laser. Peak integration used for I_{rel}.

Transient Absorbance Spectrometer. The change in sample absorbance following millisecond flash or microsecond laser photolysis was measured using the apparatus previously described[37c] and diagrammed in Figure 1. Figure 3 shows a kinetic trace from which the quantum yield was measured. At least 100 points were taken before the absorbance decreased appreciably. Transient absorbance values were calculated from voltage excursions as previously described.[39]

When using the photographic flash, the average of 5–10 voltage traces was used to evaluate the change in absorbance of the sample at each flash intensity (as described below). The same treatment was used with the laser, but the variation in flash intensity of the laser required that each voltage trace be stored and the absorbance change computed for each photolytic event.

Picosecond Spectroscopy. The ring laser system for photolyzing (0.5 ps) and observing spectra on 1–2 ps intervals is described elsewhere.[9b] Solutions for picosecond spectroscopy were made up as described above and flowed through the cell at such a rate that repeated photolysis of the same sample was avoided.

Results

Spectroscopic Properties. Reactions of the nitric oxide complex of the five-coordinate heme, (1-MeIm)Fe, were studied by

(35) Badger, G. M.; Jones, R. A.; Laslett, R. L. *Aust. J. Chem.* **1964**, *17*, 1028–1035.

(36) Anderson, O. P.; Kopelove, A. B.; Lavallee, D. K. *Inorg. Chem.* **1980**, *19*, 2101–2107.

(37) (a) Traylor, T. G.; Tsuchiya, S.; Campbell, D.; Mitchell, M.; Stynes, D.; Koga, N. *J. Am. Chem. Soc.* **1985**, *107*, 604–614. (b) Traylor, T. G.; Koga, N.; Deardurff, L. A.; Swepston, P. N.; Ibers, J. A. *J. Am. Chem. Soc.* **1984**, *106*, 5132–5143. (c) Traylor, T. G.; Chang, C. K.; Geibel, J.; Berzinis, A.; Mincey, T.; Cannon, J. *J. Am. Chem. Soc.* **1979**, *101*, 6716–6731. (d)Traylor, T. G.; Koga, N.; Deardurff, L. A. *J. Am. Chem. Soc.* **1985**, *107*, 6504–6510.

(38) Romberg, R. W.; Kassner, R. J. *Biochemistry* **1979**, *18*, 5387–5392.

(39) Chang, C. K.; Traylor, T. G. *Proc. Natl. Acad. Sci. U.S.A.* **1975**, *72*, 1166–1170.

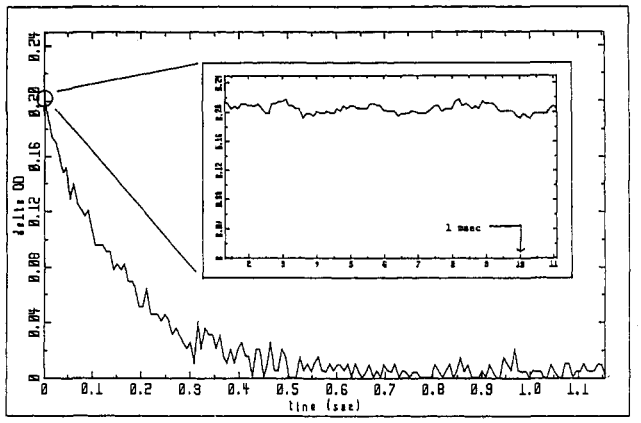

Figure 3. Sample trace showing the change in sample absorption following flash photolysis of FePP(1-MeIm)(NO) (10^{-5} M) containing NO (1 atm) measured near the Soret peak. Plot has been offset vertically from the origin to show all data points. Inset shows an expanded portion taken to calculate ΔA_i. The subsequent decay of the transient, due to bimolecular combination, is not treated in this paper.

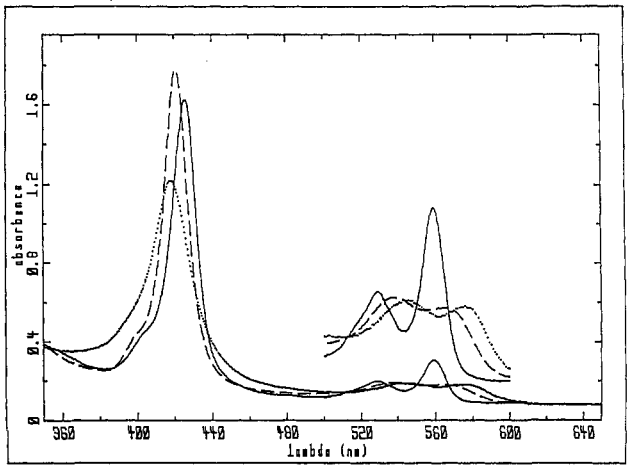

Figure 4. UV–visible absorption spectra of protoheme dimethyl ester complexes in toluene/1-methylimidazole (20%): 1-MeIm (—), CO (- - -), NO (···).

observing changes in the electronic absorption following flash photolysis. The spectra of heme compounds are highly sensitive to changes in ligation and are useful tools in the determination of sample composition. Typical absorption spectra of the CO, NO, and 1-MeIm complexes of the protoheme dimethyl ester, (1-MeIm)FePPDME, in toluene are shown in Figure 4. Complete formation of the six-coordinate nitric oxide complex, (1-MeIm)FePPDME(NO), was monitored in this way. From these spectra, it is apparent that the greatest difference in absorbance occurs in the violet (or Soret) region. During the course of a reaction, changes in sample absorbance in this region were used to determine the extent of ligand dissociation following photolysis and trapping of the photoproduct as the six-coordinate base or bis-base complex, FePPDME(1-MeIm)$_2$.

Quantum Yields. Photorelease quantum yields were determined using eq 3,

$$QI_{rel} = -\ln[1 - \Delta A(I)/\Delta A_{max}] \qquad (3)$$

where $\Delta A(I)$ is the observed change in absorbance for a flash with intensity I, ΔA_{max} is the change following full photolysis, and Q is a constant proportional to the quantum yield for photodissociation. In most cases, the value of A_{max} was taken from the static difference spectrum; however, it was sometimes necessary to calculate the value of A_{max} from a least-squares fit to the above equation. This minimized curvature of the line.[25,40-42]

(40) Bevington, P. R. *Data Reduction and Error Analysis for the Physical Sciences*; McGraw-Hill Book Co.: New York, 1981; pp 101–106.

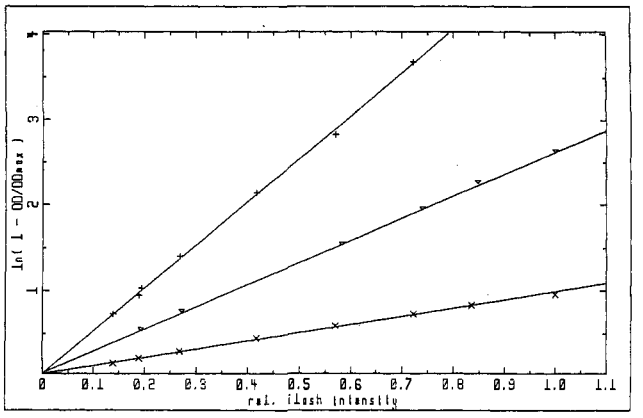

Figure 5. Plot of ligand photorelease, fit to eq 3, for mesoheme dimethyl ester complexes in toluene/1-MeIm (20%) at 20 °C. Conditions: [heme] = 5×10^{-6} M, [ligand] = 10^{-4} M. Flash source: photographic flash with 440-nm cutoff filter. (+): FeMPDME(1-MeIm)(CO). (▽): FeMPDME(1-MeIm)(*t*-BuNC). (×): FeMPDME(1-MeIm)(NO).

The error was caused by the difference in bandwidths of the analysis beams in the static and transient spectrophotometers. A plot of the right side of eq 3 versus relative flash intensity of the source yielded a straight line with slope Q. Using a monochromatic flash, Q can be defined using eq 4,

$$Q = \Phi\epsilon i \qquad (4)$$

where i is the photon flux of the flash, ϵ is the extinction coefficient of the sample, and Φ is the photorelease quantum yield.[25] The problem of determining Φ from eq 4 may be simplified in three ways. First, Φ for these compounds has been found to be wavelength independent,[25,42,43] so the use of broad-band excitation does not further complicate matters. Second, integration of the absorbance profile of each sample is avoided by evaluation of the quantum yield relative to that of a known standard[44] (carboxymyoglobin, $\Phi = 1.0$).[45] Third, evaluation of the relative quantum yields of any two samples was performed with the same light source to eliminate differences in output intensity or wavelength. The slope of the line which best fit a plot of the right side of eq 3 versus the relative intensity of the flash was used without further correction to determine the quantum yield of photodissociation relative to carboxymyoglobin.

Plots of eq 3 are shown in Figure 5 for the photographic flash. The effects of viscosity changes were studied in two solvent systems, one polar and one nonpolar. Figure 6 shows plots of eq 3 for photolyses of alkylimidazole–heme–NO complexes in both toluene and the more viscous solvent, Nujol. Figure 7 shows similar plots for photolyses in aqueous glycerol solutions having different viscosities. In both solvent types, the quantum yield decreases as viscosity increases.

Steric effects on quantum yields for NO photolyses were investigated with increasingly sterically-hindered cyclophane hemes (as judged by their rates and equilibria of reaction with carbon monoxide or *tert*-butyl isocyanide). Plots of eq 3 for hindered and unhindered model compounds are shown in Figure 8. As the steric effect increases, the quantum yield increases slightly.

Picosecond Spectroscopy. Photolysis of the 1-methylimidazole–protoheme–NO complex in 1-methylimidazole (30% in

(41) Other researchers[25,42] have used this reiterative linear-regression technique and instead included the constraint that the intercept of the theoretical line be zero at $I = 0$.

(42) Sanford, M. A.; Swartz, J. C.; Phillips, T. E.; Hoffman, B. M. *J. Am. Chem. Soc.* **1980**, *102*, 4492–4499.

(43) Saffran, W. A.; Gibson, Q. H. *J. Biol. Chem.* **1977**, *252*, 7955–7958.

(44) Our findings agree with those of previous workers,[25] who reported that the slight differences in extinction profiles between the NO complexes and Mb–CO did not significantly change the values for the quantum yield when using an actinic source.

(45) Bücher, T.; Kaspers, J. *Biochim. Biophys. Acta* **1947**, *1*, 21–34.

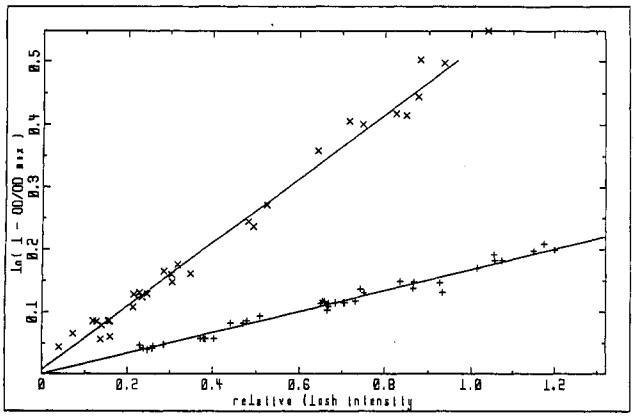

Figure 6. Plots of ligand photorelease, fit to eq 3, for NO complexes of mesoheme dimethyl ester in toluene and Nujol at 20 °C. Conditions: [heme] = 5×10^{-6} M; [ligand] = 10^{-4} M. Flash source: Phase-R pulsed-dye laser. (+): FeMPDME(1-MeIm)(NO) in toluene/20% 1-MeIm; (×): FeMPDME(1-$C_{18}H_{37}$Im)(NO) in Nujol/10% $CHCl_3$ containing *N*-octadecylimidazole (0.3 M).

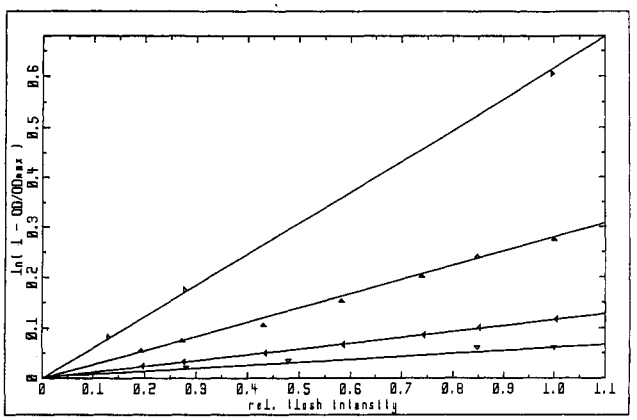

Figure 7. Plot of ligand photorelease, fit to eq 3, for NO complexes of protoheme in glycerol/water mixtures at 20 °C. Conditions: [heme] = 5×10^{-6} M; [ligand] = 10^{-4} M; solutions prepared in phosphate buffer (pH 9, 0.1 M) with 1-MeIm (30%). Flash source: photographic flash with 440-nm cutoff filter. FePP(1-MeIm)(NO) in: (▽) 0% glycerol; (△) 18% glycerol; (◁) 35% glycerol; (▽) 70% glycerol.

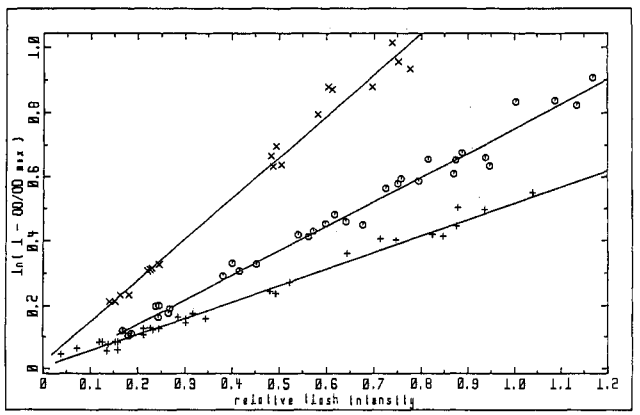

Figure 8. Plot of ligand photorelease, fit to eq 3, for NO complexes of heme in toluene/1-MeIm (20%) at 20 °C. Conditions: [heme] = 5×10^{-6} M; [ligand] = 10^{-4} M. Flash source: Phase-R pulsed-dye laser. (+): FeMPDME(1-MeIm)(NO). (○): 1-MeIm(NO)adamantane-6,6-cyclophane heme. (×): (1-MeIm)(NO)pyridine-5,5-cyclophane heme.

water) is shown in Figure 9. The rate constant for the decay is about 4×10^{10} s^{-1}, and the return is about 90%.

Discussion

The very low quantum yield for photolysis of myoglobin–NO (0.001)[30] and the low value for 1-methylimidazole–protoheme–NO (0.07)[25] photolysis have been attributed to cage return. This has been confirmed by picosecond spectroscopy studies of myoglobin–NO.[29] Table I shows the quantum yields for photolyses of 1-methylimidazole–heme–ligand complexes of various hemes. Several conclusions can be drawn.

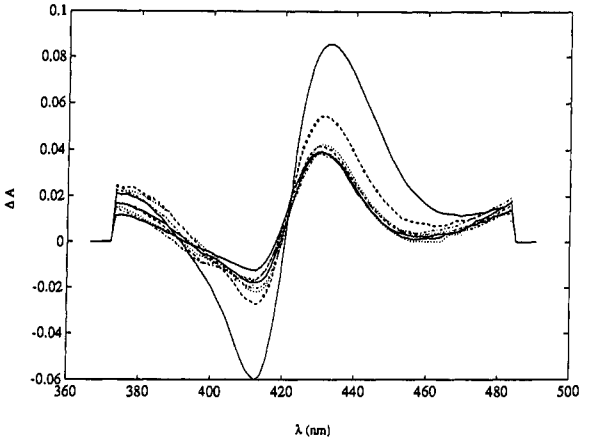

Figure 9. Picosecond transient absorption difference spectrum for (1-methylimidazole)–hemin–(NO) in water/1-MeIm (30%) saturated with NO (1 atm). Solutions prepared in 1-MeIm (30% v/v)–tris buffer (pH 9, 0.1 M). Recordings taken at 10-ps intervals.

Table I. Quantum Yields for Photodissociation of Ligands from Hemes[a,b] at 20 °C

heme	solvent	ligand	Φ[c]
(1-MeIm)mesoheme[d]	toluene[e]	CO	1.00 ± 0.04
	toluene[e]	*t*-BuNC	0.51 ± 0.02
	toluene[e]	NO	0.19 ± 0.01
(1-MeIm)protoheme[d]	toluene[e]	NO	0.21 ± 0.01
(1-MeIm)*meso*-tetraphenylheme	toluene[e]	NO	0.25 ± 0.02
(1-MeIm)*meso*-tetramesitylheme	toluene[e]	NO	0.21 ± 0.01
(1-MeIm)protoheme	H_2O[f]	CO	1.00 ± 0.05
	H_2O[f]	NO	0.077 ± 0.003
	H_2O[g]	NO	0.07

[a] Relative to carboxymyoglobin. [b] [Mb] = 5×10^{-6} M in bis/tris (pH 7, 0.05 M) in NaCl (0.1 M), [heme] = 5×10^{-6} M, [CO] = 10^{-4} M, [NO] = 10^{-4} M. [c] Using photographic flashgun. [d] The dimethyl ester. [e] Containing 1-MeIm (20%). [f] In phosphate buffer (pH 9, 0.1 M) containing 1-MeIm (30%). [g] Containing 1-MeIm (20%), ref 25.

As previously observed, the quantum yield for photolysis of BHmCO is approximately 1.00, while that for *t*-BuNC is 0.53.[17b] Both are consistent with picosecond measurements[6a,9d] and demonstrate a much larger geminate return for *tert*-butylisocyanide.

Heme Structure and Solvent Polarity Effects. The quantum yield for NO photolysis is independent of the heme structure. Differences in electronic effects between mesoheme, protoheme, and tetraphenylheme do not affect quantum yields. However, solvent effects seem to be significant. Cage returns in aqueous solutions differ greatly from those in toluene solutions. The aqueous solution of 1-methylimidazole is not sufficiently viscous to account for the decreased quantum yield. Therefore, we suggest that a more polar solvent decreases the quantum yield. It is possible that the bound state of NO, like O_2,[46] is hydrogen-bonded and that this hydrogen bond is maintained in the contact pair.

This hydrogen-bonding could also be significant in proteins. Romberg and Kassner[38] noted that $K^{NO}/K^{CO} = 16\,000$ for myoglobin and 2100 for 1-MeIm–protoheme–ligand. They attributed these results to differences in steric effects. Having ruled out such steric differentiation effects, we suggested that polar or H-bonding effects could account for this difference.[37a] Hydrogen-bonding might be much stronger in myoglobin than in the protoheme complex. The dependence of this ratio on solvent

(46) Park, K. D.; Guo, K.; Adebodun, F.; Chiu, M. L.; Sligar, S. G.; Oldfield, E. *Biochemistry* **1991**, *30*, 2333–2347.

Table II. Solvent Viscosity Effects on the Quantum Yields for Photodissociation of Nitrosylhemes[a] at 20 °C

heme	solvent	Φ
(1-MeIm)protoheme[b]	H_2O[c]	0.077 ± 0.003
	18% glycerol/H_2O[c]	0.035 ± 0.001
	35% glycerol/H_2O[c]	0.014 ± 0.001
	70% glycerol/H_2O[c]	0.007 ± 0.001
(1-MeIm)mesoheme[d,e]	toluene[f]	0.20 ± 0.01
(1-$C_{18}H_{37}$-Im)mesoheme[d,e]	Nujol[g]	0.064 ± 0.002

[a] Relative to carboxymyoglobin. [b] Source: photographic flash with 440-nm cutoff filter. [c] Aqueous solution of phosphate buffer (pH 9, 0.1 M) with glycerol and 1-MeIm (30%, v/v). [d] Mesoheme dimethyl ester. [e] Source: Phase-R pulsed-dye laser. [f] Containing 1-MeIm (20%). [g] Composed of *N*-octadecylimidazole (0.3 M) in Nujol containing $CHCl_3$ (10%).

Table III. Distal Side Effects on the Quantum Yields for Photodissociation of Nitrosylhemes[a] at 20 °C

heme	solvent	Φ[b]	k_B^{CO} (M^{-1} s^{-1})	$k_B^{O_2}$ (M^{-1} s^{-1})
(1-MeIm)mesoheme[c]	toluene[d]	0.20 ± 0.01	1.1×10^{7}[r]	8.4×10^{7}[e]
(1-MeIm)anthracene-7,7-cyclophane heme	toluene[d]	0.23 ± 0.01	6.0×10^{6}[f]	6.5×10^{7}[f]
(1-MeIm)adamantane-6,6-cyclophane heme	toluene[d]	0.29 ± 0.05	9.2×10^{3}[s]	1.5×10^{5}[s]
(1-MeIm)pyridine-5,5-cyclophane heme	toluene[d]	0.49 ± 0.06	6.0×10^{2}[s]	1.1×10^{4}[s]

[a] Relative to carboxymyoglobin. [b] Flash source: Phase-R pulsed-dye laser. [c] Mesoheme dimethyl ester. [d] Containing 1-MeIm (20%). [e] See ref 37b. [f] Solvent = benzene; see ref 37a. [g] See ref 37d.

polarity is not known, although polar solvents greatly decrease the K^{CO}/K^{O_2} ratio.[47,48]

Viscosity Effects. Quantum yields were determined in aqueous solutions having different concentrations of glycerol—up to 70% glycerol/30% 1-methylimidazole. These data, along with the corresponding data for the viscous hydrocarbon, Nujol, are shown in Table II. The quantum yield decreases by a factor of 10 as the solvent changes from 70% water/30% 1-methylimidazole to 70% glycerol/30% 1-methylimidazole. The polarity change is not large, but there is a major change in viscosity. Similarly, changing from toluene to Nujol, which does not increase the viscosity as much as does the change to glycerol, lowers the quantum yield by more than a factor of 3.

Both of these observations provide evidence for NO cage return in these systems. The question as to whether the 0.07 quantum yield for dissociation is itself entirely due to 93% geminate recombination can be answered with picosecond spectroscopy. The picosecond return in Figure 9 indicates a quantum yield for escape of about 0.1, assuming 100% initial dissociation, consistent with the quantum yield of 0.077 determined by slow-photolysis methods. We conclude that BHm–NO, like other ligand complexes, photolyzes with a quantum yield near 1.00 and that geminate recombination greatly decreases the quantum yield observed for dissociation on slower time scales, as was previously suggested.[25,49-51]

Steric Effects. We have previously studied the picosecond spectroscopy of (alkylimidazolyl)adamantanecyclophane heme-(*tert*-butylisocyanide),[9c] which had a steric hindrance to ligation, reducing the overall rate of binding this ligand by 1000-fold. The geminate return, as well as the slow-photolysis quantum yield, however, was not very different from that of unhindered chelated protoheme. This provided definitive evidence that the large steric effect in this system is not in the geminate process, i.e., not in the bond-making step, but prior to that step.

Table III shows the quantum yields for NO photolysis from mesoheme and three cyclophanes (hindered hemes). The CO binding constants in this table indicate the steric effect on CO binding and presumably on NO binding as well. In this series, the equilibrium binding constant decreases by more than a factor of 10^4, while the photolysis quantum yield changes by less than a factor of 3.

This small change in quantum yield for NO photolysis, caused by the introduction of steric effects which decrease the binding constant by about 10^4, means that NO, like isocyanides, suffers this large steric effect prior to the bond-making step. The steric effect therefore resides in the diffusion process and in the formation of the contact pair. Early observations by Frauenfelder et al.[2a,f] of myoglobin–CO dynamics indicated that the kinetics of ligation in this system are largely controlled by barriers in the protein prior to the bond-making step. It thus appears that for all the ligands (CO, NO, O_2, isocyanides) in proteins and models, the "distal steric effect" is a diffusional steric effect that inhibits the formation of the contact pair. This means that this kind of steric effect differentiates ligands by size[10a] but will not differentiate diatomic ligands such as NO, CO, and O_2. There are enormous steric effects in both proteins and model systems, but there is no evidence that these involve the bond-making or bond-breaking steps.

Recently prepared "superhindered" cyclophanes, e.g., 4,4-durene heme cyclophane[52] and a 5,5,5,5-benzene heme cyclophane,[53] might display steric effects in the bond-forming step. Thus, the 4,4-cyclophane shows a CO dissociation rate of 0.7 s^{-1}, about 30 times that for an unhindered heme. This effect appears to involve heme deformation, which is known to effect the bond-breaking/making step. However, some deformation of the ligand–iron bond might also be involved. In any case, these compounds involve steric or deformational effects which are much larger than those seen in proteins and are therefore not indicators of protein behavior.

Relevance to Heme Proteins. Picosecond studies of hemoglobin–NO and elephant and whale myoglobin–NO complexes have indicated substantial picosecond return. In both myoglobins, the return was about 90% in the first 40 ps, which implies an initial geminate rate around 10^{11} s^{-1}, similar to the rate and return observed for the model system. As in the case of the isocyanides, the picosecond geminate processes in myoglobin and in models are almost identical for NO rebinding. This finding provides evidence that studies of isocyanides are relevant to the reactions of diatomic molecules with heme proteins.

Whereas the picosecond geminate process is finished in ~40 ps and represents a single decay with a rate constant around 10^{11} s^{-1}, myoglobin has a further decay after this initial decay which extends to ~100 ps. This could either represent steric effects on bond-making (k_{-1}) or on diffusion.

Because models reveal no steric effects on k_{-1}, the simplest explanation for the biphasic (or power law) behavior of myoglobin–NO is that changes in k_2 and k_{-1} are induced by the protein. This behavior has been discussed elsewhere.[23,54]

$$\mathrm{HmNO} \underset{\substack{\sim 9\times 10^{10}\\ (k_{-1})}}{\overset{h\nu}{\rightleftharpoons}} [\mathrm{Hm\ NO}] \underset{(k_{-2})}{\overset{\substack{(k_2)\\ \sim 10^{10}}}{\rightleftharpoons}} [\mathrm{Hm}\|\mathrm{NO}] \rightleftharpoons \mathrm{Hm} + \mathrm{NO}$$

Acknowledgment. We are grateful to the National Institutes of Health (Traylor, Grant HL13581) and the National Science Foundation (Magde, Grant CHE9114613) for support.

(47) Lavalette, D.; Momenteau, M. *J. Chem. Soc., Perkin Trans. 2* **1982**, 385–388.
(48) Traylor, T. G. *Acc. Chem. Res.* **1981**, *14*, 102–109.
(49) Lavalette, D.; Tetreau, C.; Momenteau, M. *J. Am. Chem. Soc.* **1979**, *101*, 5395–5401.
(50) Hoffman, B. M.; Gibson, Q. H. *Proc. Natl. Acad. Sci. U.S.A.* **1978**, *75*, 21–25.
(51) Duddell, D. A.; Morris, R. J.; Richards, J. T. *Biochem. Biophys. Acta* **1980**, *621*, 1–8.
(52) David, S.; James, B. R.; Dolphin, D.; Traylor, T. G.; Lopez, M. A., manuscript in preparation.
(53) Kim, K.; Ibers, J. A. *J. Am. Chem. Soc.* **1991**, *113*, 6077–6081.
(54) Walda, K. N.; Liu, X. Y.; Sharma, V. S.; Magde, D., submitted for publication.